XPS and TPR Studies of Nitrided Molybdena−Alumina

Kenichiro Hada, Masatoshi Nagai,* and Shinzo Omi

Graduate School of Bio-Applications and Systems Engineering, Tokyo University of Agriculture and Technology, 2-24, Nakamachi, Koganei, Tokyo 184-8588, Japan

Received: October 12, 1999; In Final Form: December 30, 1999

The relationship between the surface molybdenum species and adsorbed nitrogen species on nitrided 1.0−18.7% MoO_3/Al_2O_3 was elucidated by XPS and temperature-programmed reduction (TPR). The MoO_3/Al_2O_3 samples were nitrided by temperature-programmed reaction with NH_3. From the XPS analysis, Mo^{3+} and Mo^{4+} ions were predominant on the surface of the nitrided Mo/Al_2O_3 samples. From the TPR measurement, the ammonia desorption was due to nitrogen species adsorbed on alumina. The nitrogen desorption was due to two kinds of nitrogen desorption from the structures of γ-Mo_2N and β-$Mo_2N_{0.78}$ and four kinds of nitrogen desorption from NH_X species adsorbed on MoO_2, Mo^{3+} ion (γ-Mo_2N), Mo^{2+} ion (molybdenum nitride on alumina such as highly dispersed molybdenum nitride), and alumina.

Introduction

Recently, molybdenum nitrides and carbides have been reported to have high activities for hydrodesulfurization and hydrodenitrogenation.[1−18] A nitrided Mo/Al_2O_3 catalyst was reported to be about 3 times more active than the sulfided and reduced Mo/Al_2O_3 catalysts in the HDN of carbazole[4] and pyridine.[7] Furthermore, the alumina-supported molybdenum nitrides were more active than sulfided Mo/Al_2O_3 catalysts for the HDS's of thiophene, benzothiophene and dibenzothiophene[6,8,9,12] and also to be extremely selective for the C−S bond breakage of dibenzothiophene to form biphenyl.[6] To elucidate the relationship between the properties of unsupported molybdenum nitrides and the activities in hydrotreating reactions, characterization has been carried out to study the adsorption/desorption of CO[1,12,16−20] and O_2, [3,7,12] TPR,[12,14−16,21] XRD,[2,3,10,14−16,19,22] XPS,[3,10,11] and NEXAFS.[23,24] The molybdenum and adsorbed nitrogen species on the unsupported molybdenum nitrides after nitriding have been studied for understanding of the active sites for the reactions. However, characterization of the nitrided molybdena-alumina rather than the unsupported molybdenum nitrides is not fully understood; whether low loading molybdenum oxides on Al_2O_3 are nitrided, what is the nitriding degree of the molybdenum atom on Al_2O_3, and the relationship between the surface molybdenum species and adsorbed nitrogen species on the nitrided molybdena−alumina. Temperature-programmed reduction with hydrogen has been used as a good technique for determining the surface properties and structures of reduced and sulfided Mo/Al_2O_3 catalysts.[25−28] Moulijin and co-workers[27,28] reported the distribution of sulfur species on supported molybdenum sulfide catalysts during TPR and temperature-programmed sulfiding and related them to molybdenum species on the surface, such as a coordinately unsaturated molybdenum atom. For unsupported nitrided samples, the distribution of molybdenum species was elucidated based on the release of nitrogen during TPR. In previous papers,[14−16] the combination of TPR and XRD enlightened the relationship between nitrogen desorption and the structure of molybdenum nitrides of the samples; γ-Mo_2N was not changed while desorbing ammonia and nitrogen below 1000 K, and γ-Mo_2N was changed to Mo metal via β-$Mo_2N_{0.78}$ while desorbing nitrogen above 1000 K during TPR. Also, several nitrogen components for nitrogen desorption were deconvoluted and related to the molybdenum species of the samples. Wei et al.[21] reported two kinds of adsorbed nitrogen on molybdenum nitrides; weakly adsorbed NH_X species released as ammonia during TPR and strongly adsorbed NH_X species as nitrogen. Bell and co-workers[23] studied the dynamics of NH_3 desorbed on γ-Mo_2N using NMR experiments and reported that NH_3 adsorbed stably up to 473 K, but the dehydrogenation of adsorbed NH_2 released NH and released nitrogen and hydrogen with increasing temperature. Also reported was the adsorption of NH_3 on the surface of Mo(100)-c(2×2)N which led to the formation of γ-Mo_2N (200) while decomposing as NH_2 and NH species.[29] However, it is not fully understood how surface NH_X species adsorbed on molybdenum nitride on alumina are reacted with hydrogen to desorb nitrogen and/or ammonia from nitrided molybdena−alumina.

On the other hand, the XPS technique provided detailed information on the oxidation states of molybdenum species by a deconvolution of the broad spectra of XPS Mo 3d for the nitrided molybdena−titania and −alumina with low molybdenum loading.[11,30,31] For the nitrided 12% Mo/TiO_2, Mo^{2+} and Mo^{3+} were major species at nitriding temperatures of 973 and 1073 K, but Mo^0 was predominant for the 1173 K-nitrided sample. Hercules and co-workers[32,33] reported the distribution of molybdenum oxidation states for 8 wt % Mo/Al_2O_3 and Mo/TiO_2 as a function of the reduction temperature with hydrogen. Mo^0 and Mo^{2+} were most noticeable for the 973- and 1173 K-reduced samples, respectively. Oliveros et al.[34] studied the distribution of molybdenum ion on the surface with molybdenum loading and reported that Mo^{6+} was outstanding for the 773 K-reduced 1.7% Mo/Al_2O_3 but Mo^{4+} and Mo^{5+} for 13.0% Mo/Al_2O_3. Thus, the oxidation states of molybdenum species varied with molybdenum loading and reduction temperature. This study focuses on (1) whether molybdenum oxides of the nitrided 1.0−18.7 wt % MoO_3/Al_2O_3 are nitrided on the surface, (2) the estimation of the nitriding degree of molybdenum by N/Mo ratios calculated from the TPR and XPS measurements, (3) what kinds of molybdenum species are related to the

* To whom correspondence should be addressed. Tel and Fax: +81-(42)-388-7060. E-mail: mnagai@cc.tuat.ac.jp.

10.1021/jp993631s CCC: $19.00
Published on Web 02/11/2000

TABLE 1: Composition and BET Surface Area of Samples

sample	Mo content[a]/wt % MoO_3	$S_{BET}/m^2\ g^{-1}$
Mo(0)*D*	0.0	177
Mo(1)*D*	1.0	178
Mo(4)*D*	4.8	189
Mo(6)*D*	6.6	177
Mo(8)*D*	8.5	172
Mo(11)*D*	11.6	171
Mo(18)*D*	18.7	169
Mo(100)*D*	100	96[b]

[a] Mo content was determined by atomic absorption spectroscopy. [b] The sample weight was weighted after BET measurement using an Omnisorp 100 CX. When 97.1 wt % MoO_3/Al_2O_3 nitrided at 973 K was weighted before the measurement with a manual apparatus (Shibata P-700), the BET surface area was 39 m^2g^{-1}.[16]

adsorbed NH_x species on the surface of the nitrided samples using TPR, and (4) the distribution of the oxidation state of molybdenum species created on the surface in the nitriding treatment.

Experimental Section

Preparation of Nitrided Mo/Al_2O_3. Molybdena−alumina samples with several molybdenum loadings were prepared by impregnation of γ-Al_2O_3 (JRC-AlO-4, Reference Catalyst, Catalysis Society of Japan) with aqueous solutions of ammonium heptamolybdate (Kishida Chemical Co., 99%). The solid products were dried at 373 K overnight and calcined at 773 K for 7 h in dry air. An unsupported molybdenum trioxide (Aldrich, 99.9%) was used for comparison. The MoO_3/Al_2O_3 sample was placed on a fritted quartz plate in a 10-mm i.d. quartz microreactor. A 0.2 g sample was nitrided by a temperature-programmed reaction with ammonia (99.99%): The sample was oxidized in dry air (1.11 mL s^{-1}) at 723 K for 1 h, cooled from 723 to 573 K in dry air, nitrided from 573 to 973 K (773, 873, 923, 1073, or 1173 K) at a rate of 0.0167 K s^{-1} with 1.11 mL s^{-1} of ammonia, held at this temperature for 3 h, and then cooled to room temperature in flowing ammonia. The nitrided samples were removed from the microreactor to transfer them into a glovebag exchanged with argon (99.9999%) five times and filled with argon gas. The samples were moved to an XPS prechamber for the XPS measurement without exposure to air. For the measurements of XRD, TEM, and BET surface area, the nitrided samples were passivated in 1% O_2/He (0.167 mL s^{-1}) for more than 12 h at room temperature. The contents (1.0, 4.8, 6.6, 8.5, 11.6, and 18.7 wt %) of molybdenum oxide on alumina of the samples were measured by an atomic absorption spectrometer (AA-630-01, Shimadzu Co.) after dissolving the samples in aqua regia (HCl:HNO_3 = 3:1). The BET surface area of the samples was measured at 77 K using an Omnisorp 100 CX (Beckman Coulter Co.) after the passivated samples were evacuated at 473 K for 2 h. The sample names were abbreviated: Mo(*x*)-*y*, where *x* is the Mo loading in wt %, *y* is *A*, *B*, *C*, *D*, *E*, and *F* for nitriding temperature in K, where *A*, *B*, *C*, *D*, *E*, and *F* are 773, 873, 923, 973, 1073, and 1173, respectively. For example, Mo(8)*A* denotes the 8.5 wt % molybdenum-loaded sample nitrided at 773 K and Mo(4-11)*D* denotes 4.8−11.6 wt % molybdenum loaded samples nitrided at 973 K. The molybdenum contents and abbreviations are summarized in Table 1.

TPR. The sample was heated in situ from room temperature to 1220 K at a rate of 0.167 K s^{-1} with 0.25 mL s^{-1} of hydrogen (99.9999%) after nitriding. Hydrogen was purified with an Indicating Oxitrap (G. L. Science) to remove water and oxygen. The desorbed gases were monitored using a quadrupole mass spectrometer (MSQ-150, ULVAC Co.). Ammonia and water in the desorbing gases during TPR were qualitatively analyzed at M/z = 15 and 18 using calibration curves, respectively, because they were overlapped at M/z = 17. Nitrogen was monitored by M/z = 28. Four kinds of pretreatment for the 973 K nitrided sample were performed before the TPR analysis. In the first pretreatment (TPR), the nitrided sample was kept at room temperature in flowing helium (99.9999%) for 12 h after nitriding. This first pretreatment is a standard procedure in the TPR analysis in this study. In the second pretreatment (He-TPR), the nitrided sample was purged with helium at a rate of 0.167 mL s^{-1} at 973 K for 1 h after nitriding and cooling to room temperature in a stream of helium. In the third pretreatment (N_2-TPR), the nitrided sample was purged with helium gas at 973 K for 1 h after nitriding, and then helium gas was exchanged with nitrogen gas (99.9999%) at 1.11 mL s^{-1}. The sample was cooled to room temperature in flowing nitrogen after allowing in nitrogen to flow in at 973 K for 1 h. In the fourth pretreatment (NH_3-TPR), the nitrided sample was purged with helium at 973 K for 1 h and then helium gas was switched to ammonia gas. The sample was placed in a flowing stream of ammonia (1.11 mL s^{-1}) at 973 K for 1 h and subsequently cooled to room temperature in flowing ammonia. The desorption spectra of nitrogen and ammonia during TPR were deconvoluted using an Origin package software equipped with a peak fitting module (Microcal Co.).

XPS. X-ray photoelectron spectroscopy was carried out using a Shimadzu ESCA 3200 photoelectron spectrometer with Mg Kα radiation (1253.6 eV, 8 kV, 30 mA). The experimental procedure consisted of removing the catalysts from the reactor after nitriding and transforming them in a glovebag without exposure to air. The glovebag was pumped and backfilled with purified argon three times before the catalysts were transferred to the XPS prechamber. The sample was mounted on a holder with carbon tape in the glovebag. No argon etching was done on analysis. The analysis was done typically at a pressure of 5 × 10^{-6} Pa at a scan speed of 0.33 eV s^{-1} with 0.05 eV $step^{-1}$. Al 2p (74.6 eV) was taken as a reference to correct the binding energy of the samples. The peaks of the XPS binding energies were deconvoluted to check the validity of various distribution with the correlation coefficient using the Origin package software after the analysis data were transferred from the Shimadzu ESCA 3200 to a PC data station. Curve fitting of the Mo3d peaks was accomplished using an intensity ratio of $^2/_3$ and a splitting of 3.2 eV, referred to by Hercules and coworkers.[32, 33]

XRD and TEM. The 18.7 wt % Mo/Al_2O_3 sample before and after TPR was measured by XRD. Diffraction patterns were obtained by RAD-II (Rigaku Co.) equipped with Cu Kα radiation (λ = 1.542 Å). The peaks were identified based on JCPDS card references; MoO_3(5-0508), MoO_2(32-671), γ-Mo_2N (25-1366), β-$Mo_2N_{0.78}$(25-1368), metallic Mo(42-1120), and γ-Al_2O_3 (10-425). The morphology of the samples was determined by JEM-2010 transmission electron microscopy (JEOL Co.) operating at 200 kV equipped an with energy-dispersive X-ray spectrometer (EDS). The sample was located on a copper grid and transferred to an analysis chamber in the TEM equipment.

Results and Discussion

TPR and XRD of 973 K-Nitrided Mo/Al_2O_3. The results of (A) TPR and (B) XRD spectra of Mo(18)*D* are shown in Figure 1. The XRD spectra for Mo(18)*A* are shown for comparison. The peaks of nitrogen desorption were observed

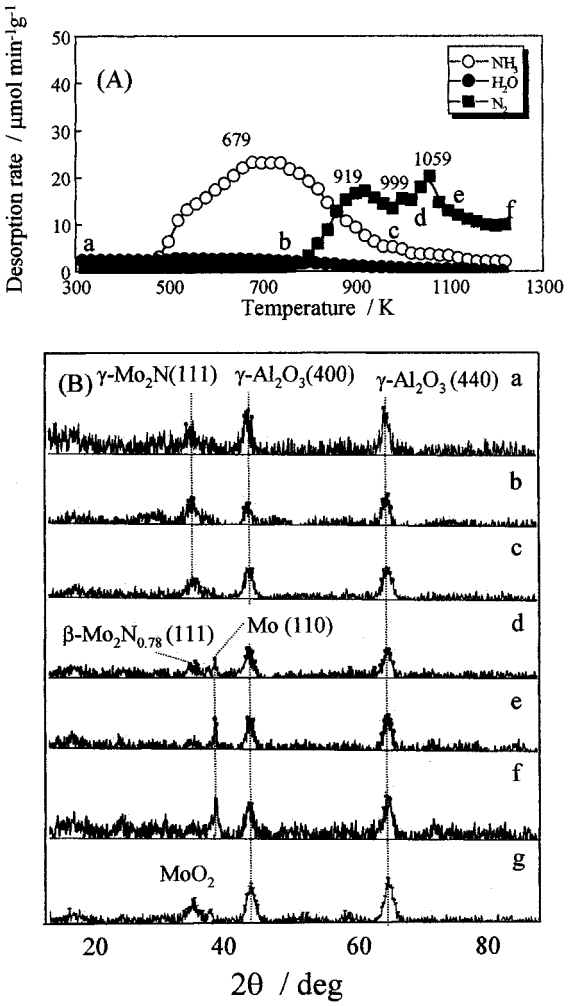

Figure 1. (A) TPR profile and (B) X-ray diffraction patterns of Mo-(18)*D*; As-nitrided Mo(18)*D* (a) at room temperature and was heated to (b) 800 K, (c) 1000 K, (d) 1020 K, (e) 1100 K, and (f) 1220 K during TPR, and (g) as-nitrided Mo(18)*A*.

at 919, 999, and 1059 K during TPR, while ammonia desorbed with a broad peak at 679 K. Water was also formed in a small amount. Mo(18)*D* sample without posttreatment (a) had γ-Mo_2N-(111), γ-Al_2O_3(400), and γ-Al_2O_3(440) reflections at 34.7°, 45.7°, and 66.3°, respectively, indicating the formation of γ-Mo_2N in the treatment of 18.7 wt % MoO_3/Al_2O_3 with ammonia at 973 K. Although the structure of γ-Mo_2N was not changed (b,c) below 980 K to retain γ-Mo_2N during TPR, -$Mo_2N_{0.78}$ (111) at $2\theta = 37.8°$ and metallic Mo(110) at 40.4° were detected for the sample heated at (d) 1020 K. The γ-Mo_2N was changed to β-$Mo_2N_{0.78}$ and metallic molybdenum from 980 to 1020 K. On further heating (e,f) above 1100 K, molybdenum metal was mainly formed together with a small amount of β-$Mo_2N_{0.78}$ while nitrogen gas desorbed during TPR. Because molybdenum metal does not contain nitrogen gas theoretically, the nitrogen desorption at 1220 K is indicative of the presence of amorphous molybdenum nitrides undetected by XRD together with crystalline molybdenum metal in the Mo(18)*D* sample. The result showed that the γ-Mo_2N in the 18.7 wt % MoO_3/Al_2O_3 nitrided at 973 K was converted to molybdenum metal through β-$Mo_2N_{0.78}$ during TPR. This is in agreement with the results for 97.1 wt % MoO_3 nitrided at 973 K via γ-Mo_2N.[14−16] Therefore, three types of adsorbed nitrogen species were released from Mo(18)*D* during TPR; (1) nitrogen gas desorbed from the surface from 800 to 1000 K, and from the structure of (2) γ-Mo_2N and (3) β-$Mo_2N_{0.78}$ from 1000 to 1050 K and above 1050 K, respectively. Moreover, ammonia eventually desorbed from the surface and as observed with a very broad peak at 679 K. This broad peak of ammonia is likely to be consistent with a weakly adsorbed NH_X species desorbed at 470−570 K during TPD reported by Wei et al.[21]

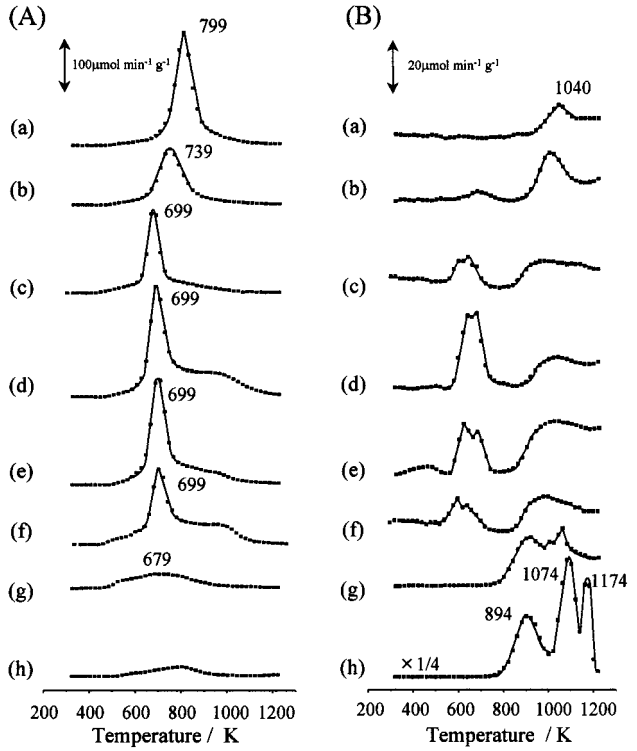

Figure 2. (A) NH_3 and (B) N_2 desorption profiles for TPR of (a) Mo-(0)*D*, (b) Mo(1)*D*, (c) Mo(4)*D*, (d) Mo(6)*D*, (e) Mo(8)*D*, (f) Mo(11)-*D*, (g) Mo(18)*D*, and (h) Mo(100)*D*.

Deconvolution of TPR Peaks. The relationship between the molybdenum species and the adsorbed NH_X species on the Mo-(1-18)*D* samples was studied, based on the desorption of nitrogen and ammonia from the samples during TPR. The desorption of (A) ammonia and (B) nitrogen during TPR for the Mo(0-18)*D* and Mo(100)*D* samples is shown in Figure 2 and summarized in Table 2. For the Mo(8)*D* sample, the peaks of ammonia and nitrogen desorption were deconvoluted, as shown in Figure 3a,b, respectively. The desorption of ammonia held the peak at temperatures of 699−799 K and a broad shoulder peak in a wide range of 500 to 1000 K in Figure 3a. The desorption amount of ammonia at temperatures of 699−799 K (A_L) decreased with increasing molybdenum loading up to 11.6 wt %. The ammonia desorption amount for Mo(18)*D* was only 3.4% less than that for Mo(0)*D* (Table 2). Therefore, the sharp peak was probably due to the release of ammonia from alumina. Furthermore, although the very broad peak at about 800 K was observed to be very wide for Mo(4-18)*D* and Mo(100)*D*, the deconvolution of the ammonia desorption was not clear (might be due to molybdenum species) and therefore could not be identified in this study.

On the other hand, six kinds of nitrogen desorption were deconvoluted with the N_L peak at 650 K and the peaks of N_{HA} to N_{HE} above 800 K for Mo(1-18)*D*. The peaks of the nitrogen desorption for the 8.5 wt % Mo/Al_2O_3 nitrided at 773−1073 K are deconvoluted (shown in Figure 4) according to the previous paper[14−16] for the sample prepared from a mixture of xerogel and heptamolybdate. The N_L peak at 650 K was observed for this sample although it has not been seen yet in the previous

TABLE 2: Desorption of Nitrogen and Ammonia during TPR for 973 K Nitrided Mo/Al_2O_3

	NH_3 desorption /μmol g^{-1}		N_2 desorption/μmol g^{-1}							
sample	A_L	correlation[a]	N_L	N_{HA}	N_{HB}	N_{HC}	N_{HD}	N_{HE}	correlation[a]	N/Mo ratio[b]
Mo(0)*D*	2197	0.991	0	0	0	125	0	0	0.971	
Mo(1)*D*	1175	0.984	19	0	75	116	55	85	0.974	3.5
Mo(4)*D*	748	0.983	111	0	118	56	95	128	0.981	1.3
Mo(6)*D*	916	0.989	289	0	79	97	100	141	0.981	1.0
Mo(8)*D*	1070	0.990	199	0	156	66	152	248	0.992	1.4
Mo(11)*D*	571	0.984	115	0	210	71	162	246	0.984	1.0
Mo(18)*D*	74	0.982	0	0	240	32	179	236	0.975	0.6
Mo(100)*D*	0	0.998	0	0	879	0	718	806	0.994	0.6

[a] Correlation coefficient. [b] Calculated from nitrogen released from Mo nitride ($N_{HD}+N_{HE}$) per Mo loading determined by atomic absorption spectroscopy.

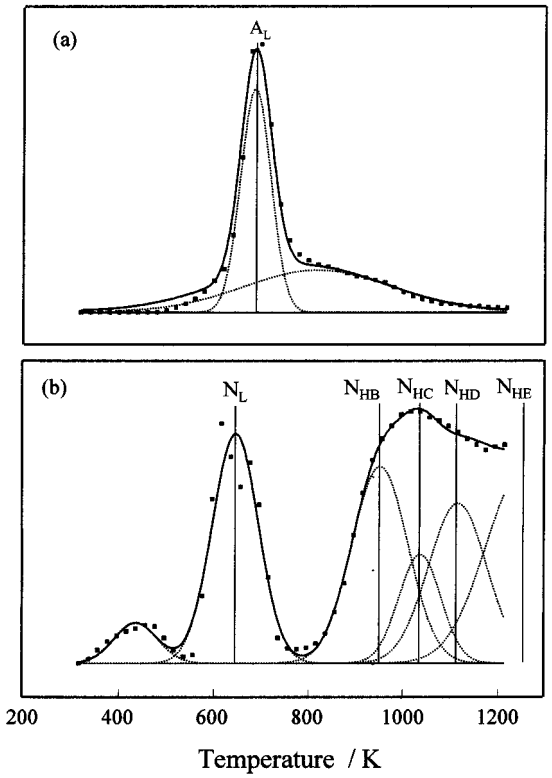

Figure 3. Peaks deconvolution of (a) NH_3 and (b) N_2 desorption in TPR profiles for the Mo(8)*D* sample.

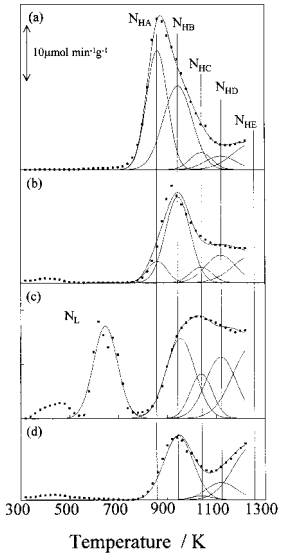

Figure 4. Nitrogen desorption for Mo(8) samples nitrided at (a) 773 K, (b) 923 K, (c) 973 K, and (d) 1073 K.

TABLE 3: Nitrogen Desorption during TPR over 8.5 wt % Mo/Al_2O_3 Nitrided at Various Temperatures

	desorption amount/μmol g^{-1}					correlation
sample	N_{HA}	N_{HB}	N_{HC}	N_{HD}	N_{HE}	coefficient
Mo(8)*A*	238	138	35	39	95	0.991
Mo(8)*B*	130	82	26	32	96	0.987
Mo(8)*C*	40	201	32	79	100	0.993
Mo(8)*D*	0	219	92	152	248	0.983
Mo(8)*E*	0	175	76	50	200	0.994
Mo(8)*F*	0	77	55	22	137	0.992

studies[14−16] on nitrided 12.5 wt % Mo/Al_2O_3 prepared by sol−gel method; ammonium heptamolybdate was dissolved in aqueous ammonium solution at 308 K. γ-Al_2O_3 xerogel was added to the ammonium paramolybdate solution, and the solution was boiled while stirring. The data are shown in Tables 2 and 3. N_{HA} is shown for Mo(8)*A* and Mo(8)*C* in Figure 4. N_L was observed with a molybdenum content from 1.0 to 11.6%, showed the maximum value at 6.6% molybdenum content and then decreased (discussed later). Mo(4-11)*D* did not have the distinct three peaks (N_{HB}, N_{HD}, and N_{HE}) as seen for Mo(18)*D* and Mo(100)*D*. N_{HB} was zero for Mo(0)*D* but increased with increasing molybdenum loading and then had a maximum for Mo(100)*D*. These results suggested that N_{HB} was ascribed to the desorption of a nitrogen species adsorbed on the molybdenum nitrides. N_{HC} desorbed from Al_2O_3 at 1040 K for Mo(0)-*D*. In Table 2, the amounts for N_{HD} and N_{HE} increased from 0.14 mmol g^{-1} for 1.0 wt % molybdenum loading to 0.415 mmol g^{-1} for 18.7 wt % molybdenum loading, that is, a 4-fold nitrogen release. The nitrogen desorption of Mo(100)*D* (1.52 mmol g^{-1}) was 4 times than that of Mo(18)*D* (0.415 mmol g^{-1}). The 4-fold nitrogen desorption was close to 5-fold molybdenum content. Therefore, the nitrogen desorption at N_{HD} and N_{HE} is due to the nitrogen structure of molybdenum nitrides; i.e., N_{HD}, nitrogen desorption from the transformation of γ-Mo_2N to β-$Mo_2N_{0.78}$ and N_{HE} from the reduction of β-$Mo_2N_{0.78}$ to Mo metal.

The desorption energy was obtained for Mo(8)*D* during TPR to determine the adsorption site of nitrogen on the molybdenum species. $\ln(\beta)-2\ln(T_P)$ is plotted against $1/T_P$ in Figure 5. The desorption energy E_a, for N_L and N_{HB} during TPR was obtained from the peak temperature (T_P) varied with increasing velocity (β). The apparent activation energies of the desorption amount at N_L and N_{HB} were 90 and 194 kJ mol^{-1}, respectively. The N_L and N_{HB} peaks were due to nitrogen adsorbed on molybdenum nitride on alumina and nitrogen from the decomposition of NH_X on the bulklike molybdenum nitrides, respectively. The desorption energy of N_L was similar to 100.3 ± 16.7 kJ mol^{-1} for the NH_3-TPD of unsupported γ-Mo_2N[35] and 92.0 kJ mol^{-1} for the NH_3-TPD of molybdenum nitride foil.[36] The N_{HB} peak is

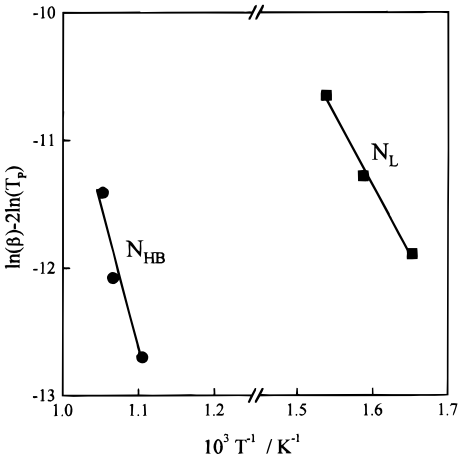

Figure 5. Desorption energy of nitrogen gas for TPR of Mo(8)*D*.

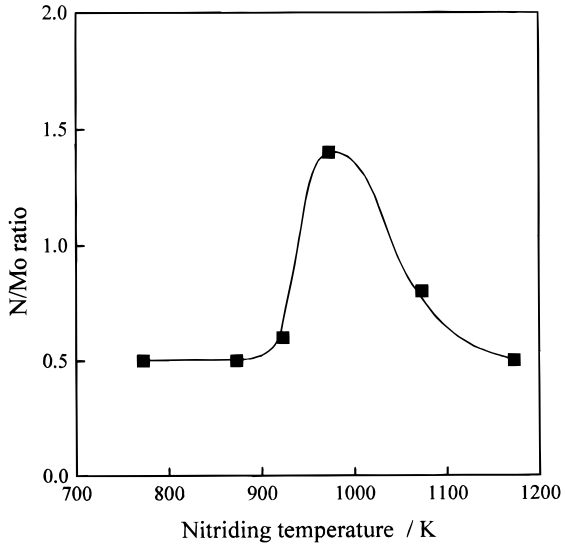

Figure 6. The N/Mo ratio obtained by TPR for 8.5 wt % Mo/Al_2O_3 as a function of nitriding temperature.

attributed to a strongly bonded NH_X on the surface of Mo_2N reported by Wei et al.[21]

N/Mo Ratio from TPR. The N/Mo ratio calculated from the $(N_{HD}+N_{HE})$/Mo ratio for Mo(18)*D* and Mo(100)*D* was 0.6 which is close to the stoichiometric N/Mo value of γ-Mo_2N, but the N/Mo ratios were 3.5 and 1.0 for Mo(1)*D* and Mo(11)-*D*, respectively. This result indicated that the 973 K-nitrided 1.0−11.6 wt % Mo/Al_2O_3 had much more nitrogen than the stoichiometric value (0.5) of γ-Mo_2N. The N/Mo ratio is plotted as a function of nitriding temperature in Figure 6. The N/Mo ratio of the 8.5 wt % Mo/Al_2O_3 sample was the desorption amounts of N_{HD} and N_{HE} for TPR divided by the number of molybdenum atoms measured by atomic absorption spectroscopy. The Mo(8)*A* had a N/Mo ratio of 0.5 from the TPR analysis, i.e., the presence of Mo_2N. However, because the XRD analysis for the Mo(18)*A* showed the composition of MoO_2 as shown in Figure 1B (g), this observation is probably due to the nitriding of MoO_2 to form molybdenum nitride with surface NH_X species during TPR while desorbing nitrogen gas.[16] Although the XRD analysis showed that Mo(8)*D* was sufficiently nitrided, the N/Mo ratio was 1.4 which was extremely larger than the stoichiometric value. The predominantly high N/Mo ratio for Mo(8)*D* is due to substantial adsorbed nitrogen and full formation of molybdenum nitrides, compared to that for Mo(8)*C* and Mo(8)*E*. Furthermore, Mo(8)*E* was 50 μmol g^{-1} due to the nitrogen desorption of N_{HD} from γ-Mo_2N to β-$Mo_2N_{0.78}$; this value is 0.3 that of the nitrogen content for the Mo(8)*D* sample without posttreatment. This result suggested that Mo(8)E mainly contained β-$Mo_2N_{0.78}$.

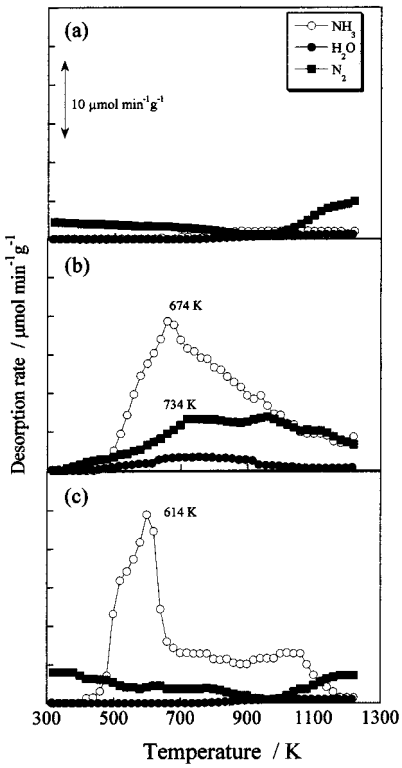

Figure 7. TPR profiles of three kinds of pretreatments after nitriding in flowing ammonia at 973 K for 3 h: (a) He-TPR, purged with helium at 973 K for 1 h and cooled to room temperature in a stream of helium, (b) NH_3-TPR, purged with helium at 973 K for 1 h, flowed in a stream of ammonia at 973 K for 1 h, and cooled to room temperature in ammonia, and (c) N_2-TPR, purged with helium at 973 K for 1 h, flowed in a stream of nitrogen at 973 K for 1 h, and cooled to room temperature in nitrogen.

Desorption Mechanism of NH_3 and N_2 during TPR. To determine how the adsorbed nitrogen and NH_X species were released as nitrogen and ammonia gases during TPR, TPR was carried out with three different pretreatments in Figure 7. For (a) He-TPR, no desorption peaks were observed below about 1000 K, because purging of the sample with helium at 973 K removed the adsorbed nitrogen and NH_X species from the surface. Nitrogen gas desorbed in a small amount above about 1000 K and contained three kinds of nitrogen (N_{HC}, N_{HD}, and N_{HE}). In Figure 7b, for the second pretreatment (NH_3-TPR), nitrogen desorbed together with ammonia. In the NH_3-TPR pretreatment, the NH_X species (NH_X, X = 1−3) on the surface reacted with hydrogen to desorb ammonia and nitrogen gases (N_L, N_{HA}, N_{HB}, and N_{HC}) during TPR mechanism 1 (Figure 8). For (c) the third pretreatment (N_2-TPR), ammonia desorption was observed at 679 K with a shoulder peak at 734 K, although nitrogen gas desorbed in a way similar to the results for He-TPR. This result was in disagreement with the desorption during He-TPR and NH_3-TPR. The peak of ammonia corresponded to the sharp peak in the spectra of Mo(4-11)*D*, as shown in Figure 2A. From the results, the adsorbed nitrogen species reacted with hydrogen to desorb ammonia but not nitrogen gas during N_2-TPR. This result showed that the adsorbed nitrogen desorbed ammonia and nitrogen but adsorbed NH_X desorbed only nitrogen. This desorption procedure of nitrogen is shown in mechanism 2 (Figure 8). To clearly understand the adsorption

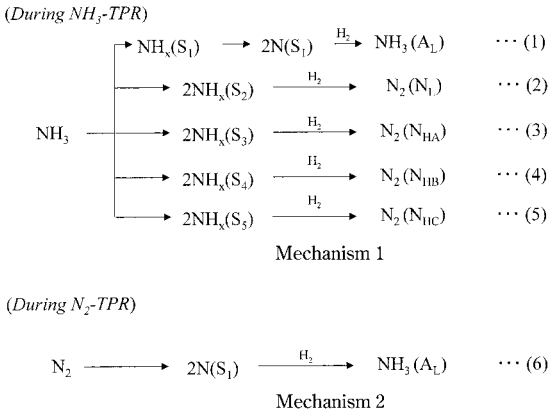

Figure 8. Desorption scheme of NH_3 and N_2 during TPR.

sites of nitrogen, S_2, S_3, and S_4 on the surface of the Mo/Al_2O_3 samples, TPR was carried out for the 8.5 wt % Mo/Al_2O_3 nitrided at 773−1073 K. In Table 3, the N_L, nitrogen species on the site S_3, was observed only for Mo(8)*D*. Note that N_L was never observed for a partially nitrided Mo(8)*C* and a not-fully reduced Mo(8)*E*, as shown in Figure 4. From the results, N_L was present on the highly dispersed γ-Mo_2N (S_2) for the 1.0−11.6 wt % Mo/Al_2O_3. Furthermore, N_{HA}, the peak at 850 K, disappeared with increasing nitriding temperature but the N_{HB} peak at 940 K became greater. This observation is in agreement with the result for the unsupported γ-Mo_2N sample containing MoO_2.[16] Therefore, N_{HA} at 850 K and N_{HB} at 940 K were due to nitrogen species on MoO_2(S_3) and γ-Mo_2N (S_4) on the surface. N_{HC}, N_{HD}, and N_{HE} were ascribed to the nitrogen species on Al_2O_3, nitrogen from the transformation from γ-Mo_2N to β-$Mo_2N_{0.78}$, and nitrogen from the reduction from β-$Mo_2N_{0.78}$ to molybdenum metal, respectively.

XPS Analysis of 973 K Nitrided Mo/Al_2O_3. The binding energies of Mo $3d_{3/2}$ and $3d_{5/2}$ for the nitrided 1.0−18.7 wt % Mo/Al_2O_3 were measured using XPS and are shown in Figure 9. The spectra of XPS Mo 3d for the nitrided Mo/Al_2O_3 samples were deconvoluted to Mo^0 (binding energy; 227.8 eV, full width half-maximum; 1.8 eV), Mo^{2+} (228.2, 2.05), Mo^{3+} (228.0, 2.12), Mo^{4+} (229.9, 2.20), Mo^{5+} (231.8, 2.29), and Mo^{6+} (233.1, 2.39), according to the XPS study of the reduced 8 wt % Mo/Al_2O_3 catalyst by Hercules and co-workers.[32] To elucidate the variation in molybdenum species in the samples with nitriding temperature, the distribution of molybdenum oxidation states was calculated as the individual Mo/Al atomic ratio divided by the total Mo/Al atomic ratios, as shown in Figure 10 and Table 4. The molybdenum oxidation states from Mo^{2+} to Mo^{6+} were observed but not Mo^0 for all the 973 K-nitrided Mo/Al_2O_3 samples. The Mo^{3+} and Mo^{4+} ions contained 80% of all the ions for the 973 K nitrided samples. Concerning the Mo^{3+} ion, the abundance of Mo^{3+} was only 10% for Mo(1)*D* but increased linearly with increasing molybdenum content from Mo(4)*D* to Mo(18)*D*. The Mo^{4+} ion was occupied at 70% for Mo(1)*D* and decreased gradually from Mo(4)*D* to Mo(18)*D*. Although the percent of Mo^{2+} was remarkably low, the distribution showed a volcano-type curve with the maximum at 6.6 wt % molybdenum content. Furthermore, the abundance of Mo^{5+} and Mo^{6+} ions was about 10 and 15% of all the samples, respectively. Thus, the molybdenum oxidation state of various Mo-loaded samples decreased with increasing molybdenum loading. This results is in agreement with the results obtained by Oliveros et al.[34] in which the average molybdenum oxidation state decreased from 5.4 to 4.6 with the increase from a molybdenum loading of 1.7 to 13.0 wt % for the 773 K-reduced Mo/Al_2O_3. Yamada et al.[32] reported that Mo^{2+} was predominant for the 973

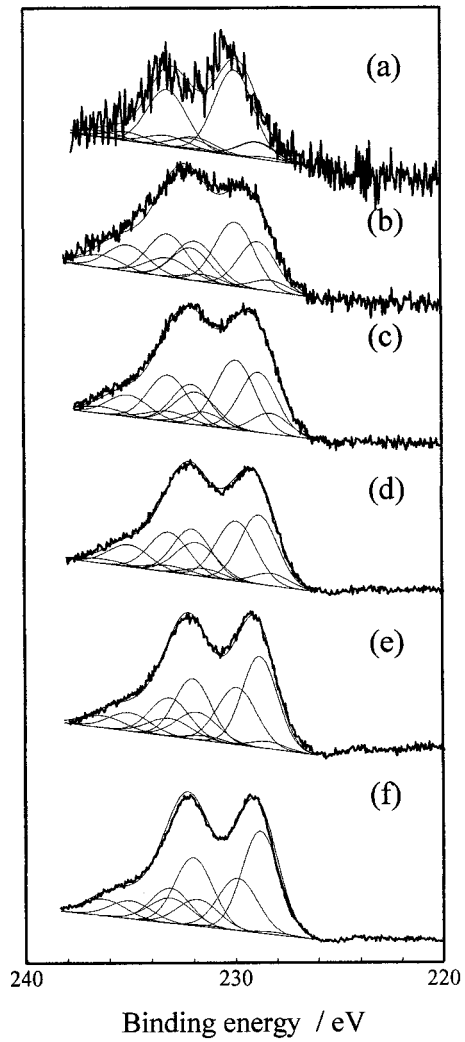

Figure 9. The binding energy of XPS Mo 3d for the 973 K nitrided Mo/Al_2O_3: (a) Mo(1)*D*, (b) Mo(4)*D*, (c) Mo(6)*D*, (d) Mo(8)*D*, (e) Mo(11)*D*, and (f) Mo(18)*D*.

TABLE 4: XPS Results of 973 K Nitride Mo/Al_2O_3 Samples

	binding energy/eV		distribution/%								
sample	Mo $3d_{5/2}$	Mo $3d_{3/2}$	Mo^{2+}	Mo^{3+}	Mo^{4+}	Mo^{5+}	Mo^{6+}	correlation[a]	Mo/Al ratio[b]	N/Al ratio[c]	N/Mo ratio[d]
Mo(1)*D*	229.9	232.9	2.1	12.6	67.1	10.6	8.0	0.956	0.03	0.10	3.3
Mo(4)*D*	229.4	232.3	5.8	26.9	33.5	20.5	12.2	0.987	0.06	0.12	2.0
Mo(6)*D*	229.3	232.2	10.0	30.2	36.2	17.7	5.8	0.997	0.07	0.11	1.6
Mo(8)*D*	229.2	232.2	5.3	38.5	30.8	17.1	7.2	0.983	0.11	0.23	2.1
Mo(11)*D*	229.2	232.2	3.0	43.7	31.4	13.5	8.5	0.979	0.16	0.32	2.0
Mo(18)*D*	229.2	232.2	1.1	48.8	26.9	14.8	8.8	0.989	0.21	0.27	1.3

[a] Correlation coefficient. [b] Mo 3d/Al 2p atomic ratio obtained by XPS. Mo/Al atomic ratio = $(S_{Mo3d}/f_{Mo3d})/(S_{Al2p}/f_{Al2p})$. Where *S* and *f* are Mo 3d in the region of 220 to 240 eV and Al 2p in the region of 70 to 82 eV and factors of sensivity of each atom and the device. [c] N 1s region (included small amounts of Mo3p)/Al 2p atomic ratio. [d] Calculated by $(N/Al)^c/(Mo/Al)^b$.

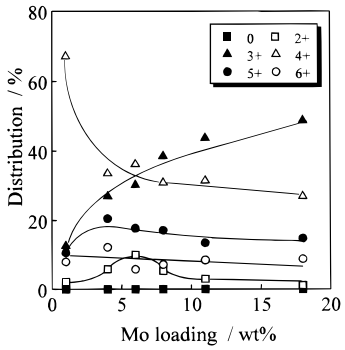

Figure 10. The distribution of molybdenum oxidation state as a function of molybdenum loading of the 973 K nitrided Mo/Al_2O_3.

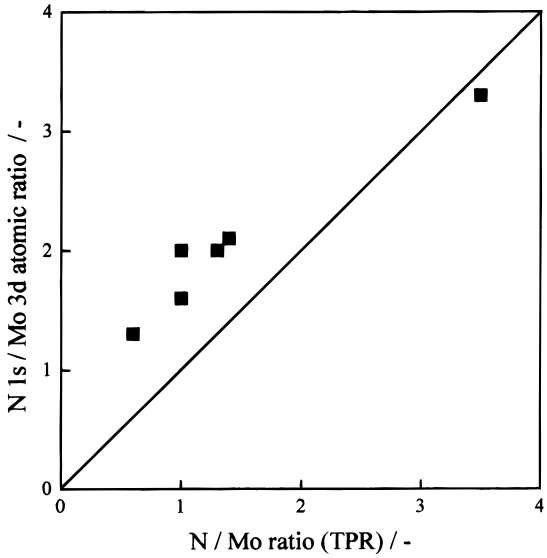

Figure 11. The relationship between the N 1s/Mo 3d atomic ratio from the XPS analysis and the N/Mo ratio from TPR for the 973 K nitrided Mo/Al_2O_3.

K-reduced 8 wt % Mo/Al_2O_3 catalyst. In the present study, Mo^{2+} ions were present at 10% of all the molybdenum species in the 6.6 wt % Mo/Al_2O_3. Greater molybdenum content of the samples weakened the interaction of the molybdenum species with alumina because of agglomerating on the sample.

Evaluation of N/Mo Ratio for Nitrided Samples. To determine whether molybdenum oxide species were nitrided for low molybdenum loaded samples, the N/Mo ratio for the 8.5 wt % Mo/Al_2O_3 sample was evaluated based on the TPR and XPS analyses. The ratios of N/Mo of Mo(1-18)*D* were calculated from the XPS data and are shown in Table 4. The atomic ratio of N/Mo was calculated from

$$\text{N/Mo atomic ratio} = [(S_{N1s}/f_{N1s})/(S_{Al2p}/f_{Al2p})]/[(S_{Mo3d}/f_{Mo3d})/(S_{Al2p}/f_{Al2p})] = (S_{N1s}/f_{N1s})/(S_{Mo3d}/f_{Mo3d}) \quad (1)$$

where S is the peak area of each atom in a binding energy region and f is the factor for the device and the sensitivity for N 1s, Al 2p, and Mo 3d in the region of 390 to 410 eV, 70 to 82 eV, and 220 to 240 eV, respectively. The N 1s spectra were overlapped with the Mo $3p_{3/2}$ spectra in the range of 390 to 410 eV; therefore, the peak area of the N 1s spectra (S_{N1s}) containing the Mo $3p_{3/2}$ spectra was calculated from the total peak area (S_{total}) minus the peak area of Mo$3p_{3/2}$ ($S_{Mo3p3/2}$).

$$S_{N1s} = S_{total} - S_{Mo3p3/2} \quad (2)$$

Because the molybdenum content ($S_{Mo3p1/2}$ and $S_{Mo3p3/2}$)/Al 2p, in the Mo/Al_2O_3 samples was not changed in the region of 390 to 430 eV before and after nitriding, the peak area of Mo $3p_{3/2}$ in the nitrided samples can be corrected by a factor (f^0_{Mo3p}) of the atomic ratio of Mo $3p_{1/2}$/Mo $3p_{3/2}$ in the 18.7 wt % Mo/Al_2O_3 oxidized at 723 K. Therefore, using the peak area of Mo $3p_{1/2}$ ($S_{Mo3p1/2}$) in the nitrided sample, $S_{Mo3p3/2}$ can be written as

$$S_{Mo3p3/2} = S_{Mo3p1/2} \times f^0_{Mo3p} \quad (3)$$

From eqs 1, 2, and 3,

$$\text{N/Mo} = [(S_{total} - S_{Mo3p1/2} \times f^0_{Mo3p})/f_{N1s}]/(S_{Mo3d}/f_{Mo3d}) \quad (4)$$

In the XPS analysis, the N/Mo ratio had the maximum for Mo-

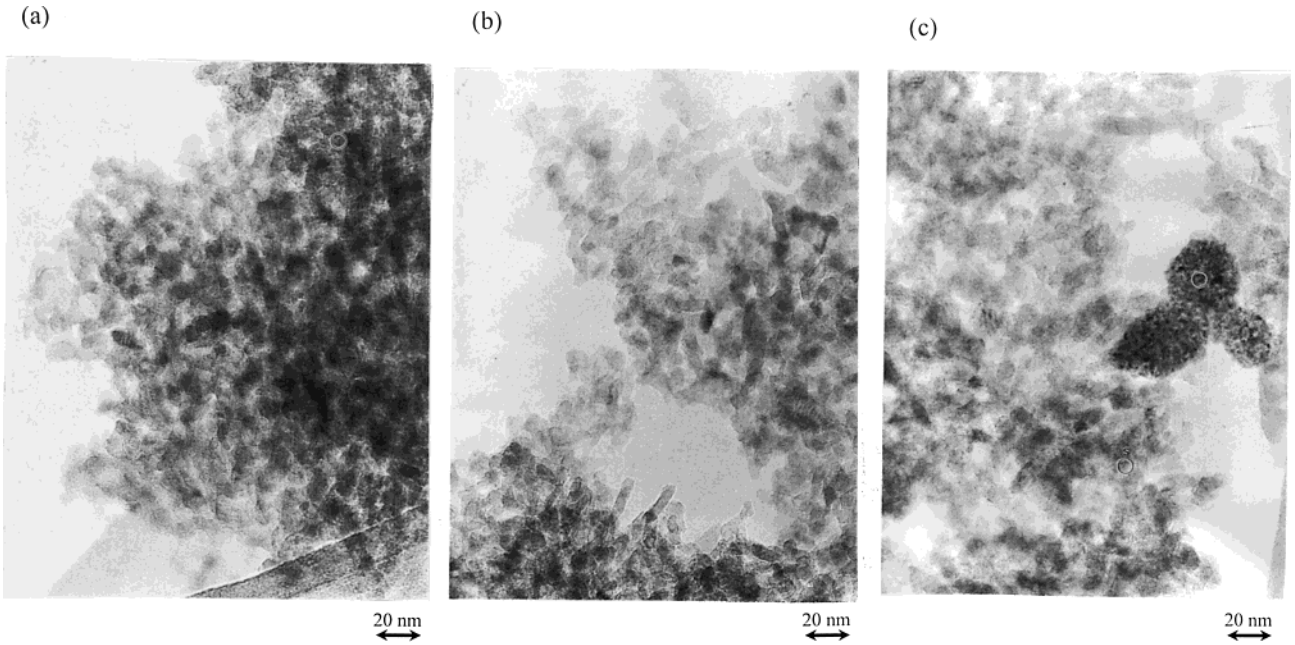

Figure 12. TEM images of the nitrided Mo/Al_2O_3 samples: (a) Mo(1)*D*, (b) Mo(8)*D*, and (c) Mo(11)*D* samples. The TEM image was recorded at a magnification of 200000×.

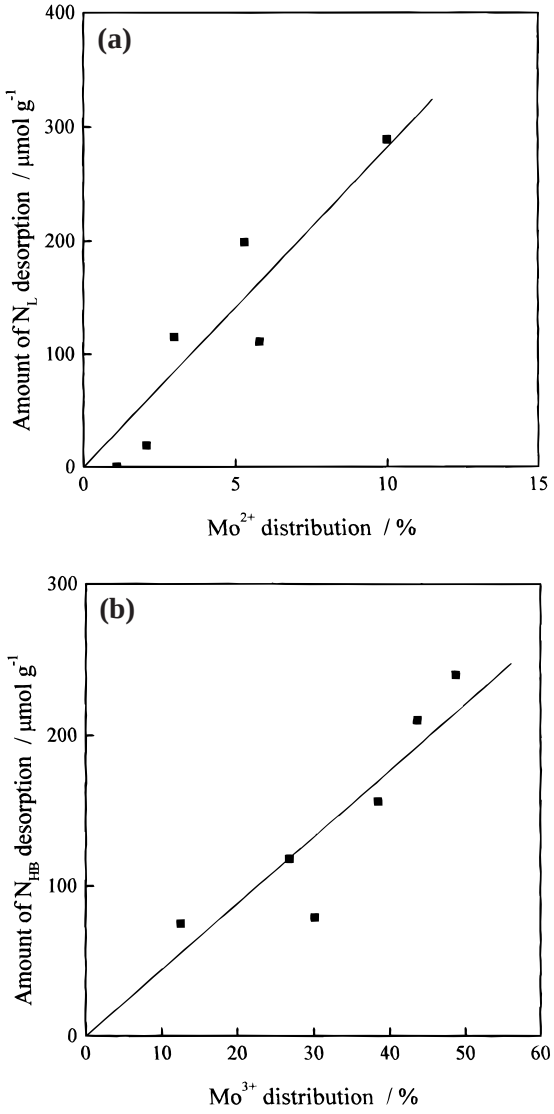

Figure 13. The relationship between the amounts of nitrogen desorption during TPR and the distribution of Mo^{X+} from the XPS analysis: (a) the N_L desorption amount as a function of the distribution of Mo^{2+} and (b) the N_{HB} desorption amount as a function of the distribution of Mo^{3+}.

(1)*D* and decreased with increasing molybdenum loading of the samples in Table 4. Both the XPS and TPR results showed that Mo(1)*D* had much nitrogen.

The relationship between the N/Mo atomic ratios from the TPR and XPS is shown in Figure 11. The N/Mo ratio from the XPS analysis was proportional to that from the TPR data by a factor of 1. The N/Mo ratio below 2 slightly deviated from a straight line due to the difference between the molybdenum content of the surface component analyzed by XPS and that of the total component of the samples (atomic absorbance analysis). Therefore, molybdenum oxides in the Mo/Al_2O_3 samples with even 1% molybdenum loading were nitrided based on both the TPR and XPS analyses.

Morphology of Nitrided Mo/Al_2O_3 Sample. The TEM images of Mo(1)*D*, Mo(4)*D*, and Mo(11)*D* are shown in Figure 12. Molybdenum and aluminum atoms were observed in all the samples from the EDS analysis. For Mo(11)*D*, the Mo/Al ratio at the L position was 9.5 times greater than that at the S position. These results indicated that molybdenum particles were uniformly presented on the surface of the 973 K nitrided 11.6 wt % Mo/Al_2O_3 sample. From the EDS analysis, the Mo/Al ratio at the L position for Mo(11)*D* was 26 times greater than that for Mo(4)*D*, but the Mo/Al ratio for Mo(4)*D* was 4 times greater than that of Mo(1)*D* at the L position. From the image of the L position, the molybdenum species of the samples up to 4.8 wt % molybdenum loading sample was not agglomerated but highly dispersed on alumina. Furthermore, Mo(11)*D* consisted of a molybdenum particle of ca. 7 and 0.2 Å at L position. Molybdenum nitrides of Mo(11)*D* were partially agglomerated to form large particles of molybdenum nitride on the surface.

Molybdenum Species Related to Surface Nitrogen Species. The relationship between the distribution of Mo^{X+} obtained from XPS and the desorption amounts of the surface nitrogen species from TPR is shown in Figure 13. Since N_{HB} is proportional to the presence of Mo^{3+}, but not Mo^{2+}, Mo^{4+}, Mo^{5+}, and Mo^{6+}, the NH_X species (N_{HB}) are located on the Mo^{3+} ion for the nitrided 1.0−18.7 wt % Mo/Al_2O_3 samples. The surface molybdenum species were mainly Mo^{3+} on the bulklike γ-Mo_2N species. On the other hand, N_L is proportional to Mo^{2+} but not to the other ions. N_L is present only on the surface of the Mo-(1-11)*D* samples and represents nitrogen species on γ-Mo_2N. Therefore, N_L is located on the Mo^{2+} ion such as highly dispersed molybdenum nitride on alumina of the Mo/Al_2O_3. Nagai et al.[31] reported that Mo^{2+} and Mo^0 were the most active in the HDS of dibenzothiophene on a nitrided Mo/TiO_2 catalyst. Mo^{2+} ions were also reported to be the most active species for the hydrogenation of benzene on reduced Mo/Al_2O_3[32] and Mo/TiO_2[33] catalysts. Furthermore, a possible observation of the doublet peaks of N_L in Figure 2B (c)−(f) would be due to nitrogen from the desorption of the NH and NH_2 species on the surface.

Conclusions

The N/Mo ratios from the XPS and TPR analyses showed that molybdenum nitrides were formed for the 973 K-nitrided Mo/Al_2O_3 with 1.0−18.7% Mo loadings. Ammonia is desorbed from nitrogen species adsorbed on the 973 K-nitrided Mo/Al_2O_3. Four kinds of nitrogen species on 973 K-nitrided Mo/Al_2O_3 desorbed as nitrogen; the nitrogen species (N_L) on highly dispersed γ-Mo_2N, the nitrogen species (N_{HA} and N_{HB}) on molybdenum species such as MoO_2 and γ-Mo_2N, respectively, and the nitrogen species (N_{HC}) on alumina, and two kinds of nitrogen gases (N_{HD} and N_{HE}) desorbed from γ-Mo_2N to β-$Mo_2N_{0.78}$ and γ-$Mo_2N_{0.78}$ to Mo metal, respectively. Molybdenum nitrides formed on 4.8−18.7 wt % 973 K-nitrided Mo/Al_2O_3 contained mainly Mo^{3+} and Mo^{4+} ions. The nitrogen at N_L is located on the Mo^{2+} ion of highly dispersed molybdenum nitride on alumina. The nitrogen desorption at N_{HB} is located on the Mo^{3+} ion of γ-Mo_2N on Mo/Al_2O_3.

Acknowledgment. We are grateful for the Grant-In-Aid for Scientific Reserch of the Ministry of Education, Grant 09555244.

References and Notes

(1) Schlatter, J. C.; Oyama, S. T.; Metcalfe, J. E.; Lambert, J. M. *Ind. Eng. Chem. Res.* **1988**, *27*, 1648.
(2) Markel, E. J.; Van Zee, J. W. *J. Catal.* **1990**, *126*, 643.
(3) Choi, J.-G.; Brenner, J. R.; Colling, C. W.; Demczyk, B. G.; Dunning, J. L.; Thompson, L. T. *Catal. Today* **1992**, *15*, 201.
(4) Nagai, M.; Miyao, T. *Catal. Lett.* **1992**, *15*, 105.
(5) Lee, K. S.; Abe, H.; Reimer, J. A.; Bell, A. T. *J. Catal.* **1993**, *139*, 34.
(6) Nagai, M.; Miyao, T.; Tuboi, T. *Catal. Lett.* **1993**, *18*, 9.
(7) Colling, C. W.; Thompson, L. T. *J. Catal.* **1994**, *146*, 193.
(8) Aegerter, P. A.; Quigley, W. W. C.; Simpson, G. J.; Ziegler, D. D.; Logan, J. W.; McCrea, K. R.; Glaizier, S.; Bussell, M. E. *J. Catal.* **1996**, *164*, 109.

(9) Dolce, G. M.; Savage, P. E.; Thompson, L. T. *Energy Fuels* **1997**, *11*, 668.
(10) Ozkan, U. S.; Zhang, L.; Clark, P. A. *J. Catal.* **1997**, *172*, 294.
(11) Park, H. K.; Lee, J. K.; Yoo, J. K.; Ko, E. S.; Kim, D. S.; Kim, K. L. *Appl. Catal. A.; Gen.* **1997**, *150*, 21.
(12) McCrea, K. R.; Logan, J. W.; Tarbuck, T. L.; Heiser, J. L.; Bussell, M. E. *J. Catal.* **1997**, *171*, 255.
(13) Nagai, M.; Irisawa, A.; Omi, S. *J. Phys. Chem. B* **1998**, *102*, 7619.
(14) Nagai, M.; Kusagaya, T.; Miyata, A.; Omi, S. *Bull. Soc. Chim. Belg.* **1995**, *104*, 311.
(15) Nagai, M.; Miyata, A.; Kusagaya, T.; Omi, S. *In The Chemistry of Transition Metal Carbides and Nitrides;* Oyama, S. T. Ed.; Blackie; London, 1996; p327.
(16) Nagai, M.; Goto, Y.; Miyata, A.; Kiyoshi, M.; Hada, K.; Oshikawa, K.; Omi, S. *J. Catal.* **1999**, *182*, 292.
(17) Oyama, S. T. *Catal. Today* **1992**, *15*, 179.
(18) Sajokowski, D. J.; Oyama, S. T. *Appl. Catal. A.; Gen*. **1996**, *134*, 339.
(19) Ranhotra, G, S.; Haddix, G. W.; Bell, A. T.; Reimer, J. A. *J. Catal.* **1987**, *108*, 24.
(20) Saito, M.; Anderson, R. B. *J. Catal.* **1980**, *63*, 438.
(21) Wei, Z.; Xin, Q.; Grange, P.; Delmon, B. *J. Catal.* **1997**, *168*, 176.
(22) Haddix, G. W.; Jones, D. H.; Reimer, J. A.; Bell, A. T. *J. Catal.* **1988**, *112*, 556.
(23) Chen, J. G. *Chem. Rev.* **1996**, *96*, 1477.
(24) Kapoor, R.; Oyama, S. T.; Frühberger, B.; Chen, J. G. *J. Phys. Chem. B* **1997**, *101*, 1543.
(25) Koerts, T.; Welters, W. J. J.; van Santen, R. A. *J. Catal.* **1992**, *134*, 1.
(26) Fastrup, B.; Muhler, M.; Nielsen, H. N.; Nielsen, L. P. *J. Catal.* **1993**, *142*, 135.
(27) Muller, B.; van Langveld, A. D.; Moulijin, J. A.; Knozinger, H. *J. Phys. Chem.* **1993**, *97*, 9028.
(28) Mangnus, P. J.; Riezebos, A.; van Langveld, A. D.; Moulijin, J. A. *J. Catal.* **1995**, *151*, 178.
(29) Bafrali, R.; Bell, A. T. *Surf. Sci.* **1992**, *278*, 353.
(30) Nagai, M.; Miyata, A.; Miyao, T.; Omi, S. *J. Jpn. Petro. Inst.* **1997**, *40*, 500.
(31) Nagai, M.; Takada, J.; Omi, S. *J. Phys. Chem. B* **1999**, *103*, 10180.
(32) Yamada, M.; Yasumaru, J.; Houalla, M.; Hercules, D. M. *J. Phys. Chem.* **1991**, *95*, 7037.
(33) Quincy, B. R.; Houalla, M.; Proctor, A.; Hercules, D. M. *J. Phys. Chem.* **1990**, *94*, 1520.
(34) Olivelos, I.; Zurita, M. J. P.; Scott, C.; Goldwasser, M. R.; Goldwasser, J.; Rondon, S.; Houalla, M.; Hercules, D. M. *J. Catal.* **1997**, *171*, 485.
(35) Colling, C. W.; Choi, J.-G.; Thompson, L. T. *J. Catal.* **1996**, *160*, 35.
(36) Lee, H. J.; Choi, J.-G.; Colling, C. W.; Mudholkar, M. S.; Thompson, L. T. *Appl. Sulf. Sci.* **1995**, *89*, 121.